Robotica (1999) volume 17, pp. 3–9. Printed in the United Kingdom © 1999 Cambridge University Press

A proposal for a wire suspended manipulator: A kinematic analysis

Tamio Arai,* Shojiro Matsumura,* Yuji Yoshimura,* Hisashi Osumi**

SUMMARY

Industrial robots have a high positioning accuracy and stiffness but their work spaces are limited because their bases are fixed to the ground. To enlarge the work spaces, this paper proposes a novel mechanism, a wire suspended manipulator with three degrees of freedom. First, the kinematics of the mechanism is derived from both force and geometric constraints. Second, the volume of the work space is numerically calculated. After the evaluation of manipulability of the wire suspended system, guidelines for designing parameters are studied.

KEYWORDS: Wire suspended manipulator; Kinematic analysis; Industrial robots.

1. INTRODUCTION

Manipulators are used extensively in industry. But their work spaces are limited because their bases are fixed to the ground. Thus, manipulators mounted on mobile vehicles,[1–3] limb mechanisms,[4] wall climbing robots[5] and brachiation robots[6] have been studied in order to improve performance.

In this study, we propose a wire suspended manipulator, which consists of a wire suspension mechanism and a conventional manipulator mechanism; an industrial manipulator is suspended under a movable mechanism like a crane, as shown in Fig. 1. The static model of the total mechanism has two passive joints at both ends of the wire and three active joints on the manipulator. This mechanism has a large work space like a crane system and has the following characteristics:

(i) When active joints move, the pose of the base of the manipulator also changes.
(ii) The pose of the base changes according to external forces applied to the end-effector.
(iii) As the manipulator is equivalent to a pendulum, vibrations are generated by the motions of the manipulator.

Kinematics includes the constraints about the equilibrium of the gravity and the applied forces. When the manipulator grasps handling objects, not only the pose but also the work space changes according to the weight of the objects. Note that the applicable forces to the outside of the mechanism are generated by using the change of the potential energy of the suspended manipulator system.

In this paper, we consider tasks around the equilibrium point; thus the control of the manipulator is only studied to position the end-effector. First, direct kinematics and inverse kinematics are derived from geometric constraints by joint angles of the manipulator and the equilibrium. The process of these formulations is similar to that of space robotics, and we can derive the Jacobian matrix like a generalized Jacobian matrix[7,8] from the equilibrium. Statics is also derived using the Jacobian matrix. Second, the guidelines of designing parameters of the manipulator are obtained by evaluating its work space and its manipulability measure as criteria.

This wire suspended manipulator works effectively when the manipulator can reach the working target from a distant high position, e.g. maintenance work in power stations and oil tanks, construction with crane control, and so forth.

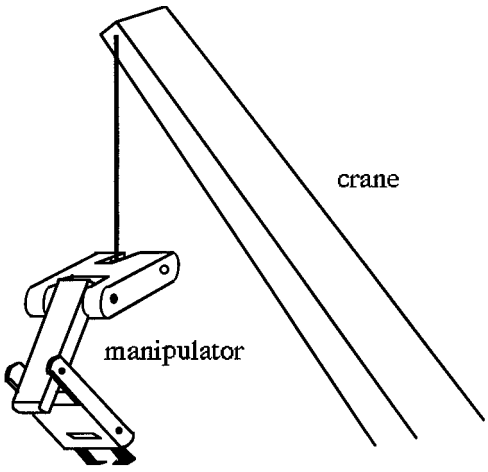


Fig. 1. A wire suspended manipulator.

* The University of Tokyo, 7-3-1, Hongo, Bunkyo-ku Tokyo 113 (Japan)
** Chuo University, 1-13-27, Kasuga, Bunkyo-ku, Tokyo 112 (Japan)

2. FORMULATION OF A WIRE SUSPENDED MANIPULATOR

2.1 Model of a wire suspended manipulator

A model of a wire suspended manipulator is illustrated in Fig. 2. The model consists of a serial link with 3 degrees of freedom, a suspension mechanism of a single wire, and a crane as a positioning device of the upper end of the wire. Assuming that the length of the end-effector is 0, i.e. the distance between the wrist joint and the tip of the hand is small enough to be neglected, the mechanism can be modeled as one with three rigid links with three active joints (θ_2, θ_3, θ_4) and two passive joints (ϕ_0, ϕ_1) at both ends of the

https://doi.org/10.1017/S0263574799000995 Published online by Cambridge University Press

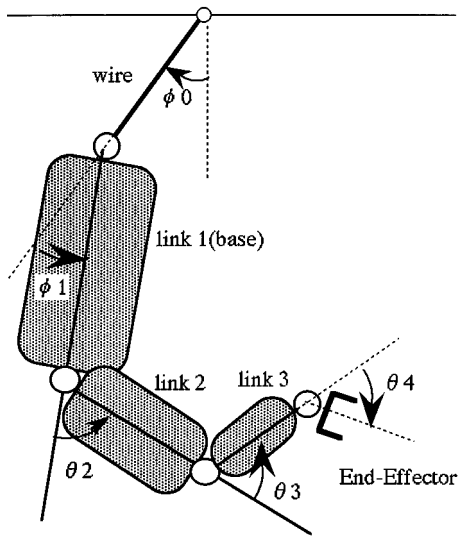


Fig. 2. A model of a wire suspended manipulator.

wire, as shown in Fig. 2. Note that the mass of the wire and its twist can be insignificant in this model.

Though the mechanism can work in a three-dimensional space, it is analyzed in a vertical two-dimensional plane so as to simplify the model. When the crane moves in three dimensions, the system has five degrees of freedom totally. The rotation about the vertical wire cannot be controlled if a single wire suspends the manipulator. In that case, the plural wiring mechanism should be introduced, as we have studied in references 9 and 10.

2.2 Kinematics of a wire suspended manipulator

Under the static condition, the orientation of the manipulator base ϕ_1 is determined by the configuration of the active joints (θ_2, θ_3, θ_4) and the external force applied to end-effector. On the other hand, the swing angle of the wire ϕ_0 can simply be calculated by the external force.

Let us define each coordinate system and each vector of the suspended mechanism as shown in Fig. 3. The coordinate system Σ_c is a reference frame, whose origin is on the crane with the x axis in a horizontal plane. The coordinate system Σ_i is a link coordinate system set on each link, whose origin is located at each joint and a direction of the axis of each link is set as their axis. $\mathbf{L}_i$ and $\mathbf{a}_i$ are the vectors that represent the position of the next link coordinate system and gravity center of each link from each link coordinate system, respectively. The letter attached on the left shoulder of the vector means that the vector is defined on the link coordinate system. With no letters, the vector is defined on the reference frame.

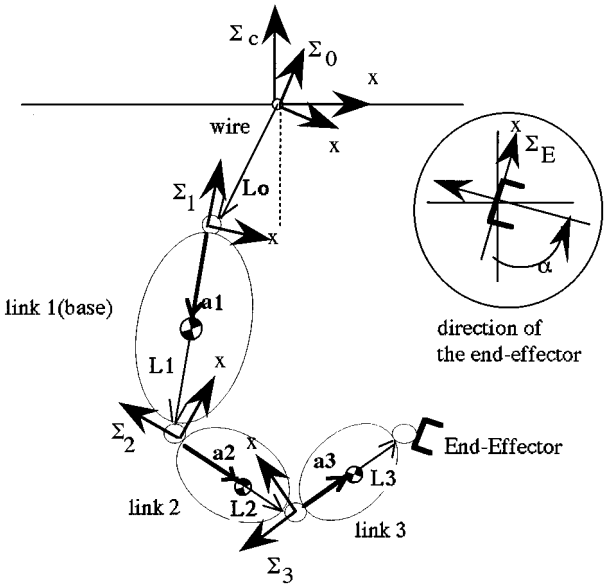


Fig. 3. Coordinate system of a wire suspended manipulator.

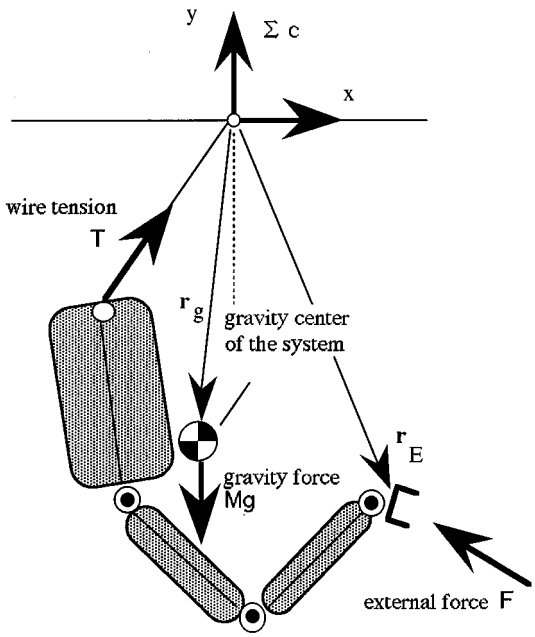


Fig. 4. A model with external force given at the end-effector.

Then, the pose of the end-effector $\mathbf{r}_E$ is obtained as

$$\mathbf{r}_E = \sum_{i=0}^{3} {}^{c}R_i \, {}^{i}\mathbf{L}_i \tag{1}$$

where ${}^{c}R_i = {}^{c}R_0 \prod_{k=0}^{i-1} {}^{k}R_{k+1}$.

The matrix ${}^{i-1}R_i$ relates the link coordinate system Σ_{i-1} to the link coordinate system Σ_i. ${}^{i-1}R_i$ is represented as:

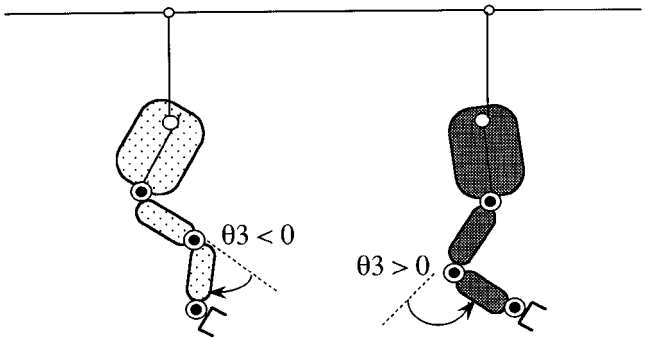


Fig. 5. An example of inverse kinematics solutions.

https://doi.org/10.1017/S0263574799000995 Published online by Cambridge University Press

Table I. Link parameters of a wire suspended manipulator

L_0 0.20 [m]		
L_1 0.20 [m]	a_1 0.10 [m]	m_1 1.61 [kg]
L_2 0.16 [m]	a_2 0.08 [m]	m_2 1.05 [kg]
L_3 0.16 [m]	a_3 0.08 [m]	m_3 1.65 [kg]

$$ {}^{c}R_0 = \begin{bmatrix} \cos\phi_0 & -\sin\phi_0 \\ \sin\phi_0 & \cos\phi_0 \end{bmatrix} \tag{2} $$

$$ {}^{i-1}R_i = \begin{bmatrix} \cos\theta_i & -\sin\theta_i \\ \sin\theta_i & \cos\theta_i \end{bmatrix} $$

As Eq. (1) includes passive joints, we need to solve the equilibrium with the gravity to calculate $\mathbf{r}_E$.

Figure 4 illustrates the static balance of the system. The equilibrium is represented as

$$ \mathbf{T} + M\mathbf{g} + \mathbf{F} = \mathbf{0} \tag{3} $$

$$ \mathbf{r}_E \times \mathbf{F} + \mathbf{r}_g \times M\mathbf{g} = \mathbf{0} \tag{4} $$

where

$$ M = \sum m_i $$

$$ \mathbf{T} = (T_x\ T_y)^T $$
$$ \mathbf{g} = (0\ -g)^T $$
$$ \mathbf{F} = (F_x\ F_y)^T $$
$$ \mathbf{r}_g = (r_{gx}\ r_{gy})^T $$
$$ \mathbf{r}_E = (x\ y)^T $$

Therefore, the passive joint ϕ_0 is calculated as

$$ \phi_0 = \tan^{-1}\left(-\frac{T_x}{T_y}\right) = \tan^{-1}\left(\frac{F_x}{Mg - F_y}\right) \tag{5} $$

Equation (5) indicates that ϕ_0 is determined by just the gravity force and the external force **F**. Next, we calculate the other passive joint ϕ_1. Component of Eq. (4) is represented as

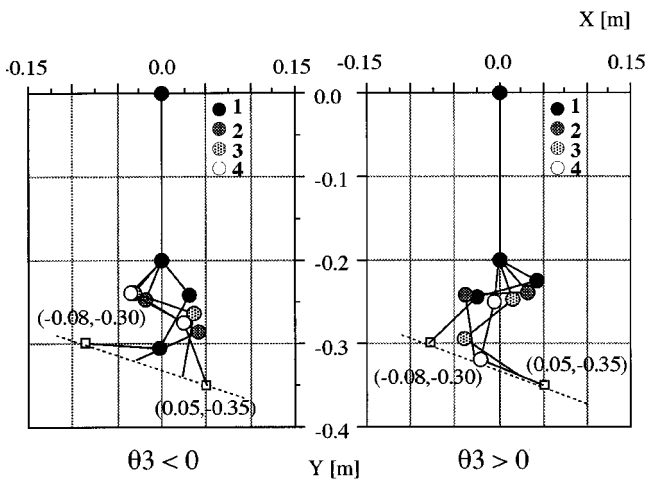


Fig. 6. Simulation results of inverse kinematics.

$$ xF_y - yF_x - Mgr_{gx} = 0 \tag{6} $$

Replacing Eq. (6) with the passive joint ϕ_0, we obtain

$$ k_1(\phi_0,\ \theta_1,\ \mathbf{F})\sin\phi_1 + k_2(\phi_0,\ \theta_1,\ \mathbf{F})\cos\phi_0 = 0 \tag{7} $$

and then the passive joint ϕ_1 is calculated as

$$ \phi_1 = \tan^{-1}\left(\frac{-k_2}{k_1}\right) \tag{8} $$

Substituting the results of the joints ϕ_0 and ϕ_1 into Eq. (1), we obtain the position and orientation of the end-effector as

$$ x = L_0S_0 + L_1S_{01} + L_2S_{012} + L_3S_{0123} \tag{9} $$

$$ y = -L_0C_0 - L_1C_{01} - L_2C_{012} - L_3C_{0123} \tag{10} $$

$$ \alpha = \phi_0 + \phi_1 + \theta_2 + \theta_3 + \theta_4 \tag{11} $$

where $S_{ijk} = \sin(\theta_i + \theta_j + \theta_k)$, $C_{ijk} = \cos(\theta_i + \theta_j + \theta_k)$.

Consequently, we can obtain the kinematics of the wire suspended manipulator.

3. INVERSE KINEMATICS OF A WIRE SUSPENDED MANIPULATOR

3.1 Derivation of Jacobian matrix

Since this mechanism includes passive joints, it is difficult to calculate the inverse kinematics analytically. Thus, we calculate the inverse kinematics iteratively using the Jacobian matrix of the joint angles against the pose of the end-effector. Let us derive the Jacobian matrix of the wire suspended manipulator; it is represented generally as Eq. (12).

$$ d\mathbf{x} = (J_\phi\ J_\theta)\begin{pmatrix} d\boldsymbol{\phi} \\ d\boldsymbol{\theta} \end{pmatrix} \tag{12} $$

$$ = J_\phi d\boldsymbol{\phi} + J_\theta d\boldsymbol{\theta} $$

where $\mathbf{x} = (x_E\ y_E\ \alpha)^T$, $\boldsymbol{\phi} = (\phi_0\ \phi_1)^T$, $\boldsymbol{\theta} = (\theta_2\ \theta_3\ \theta_4)^T$

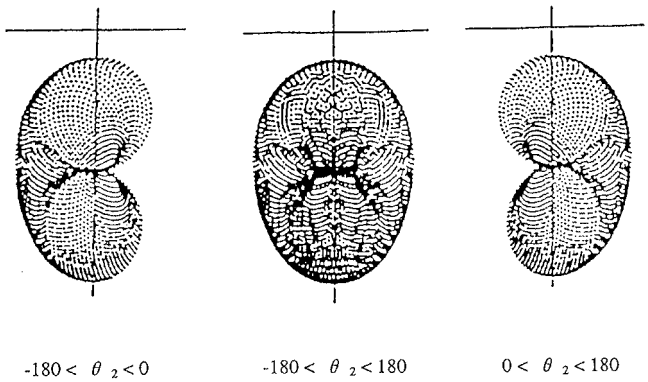


Fig. 7. Reachable space of a wire suspended manipulator.

https://doi.org/10.1017/S0263574799000995 Published online by Cambridge University Press

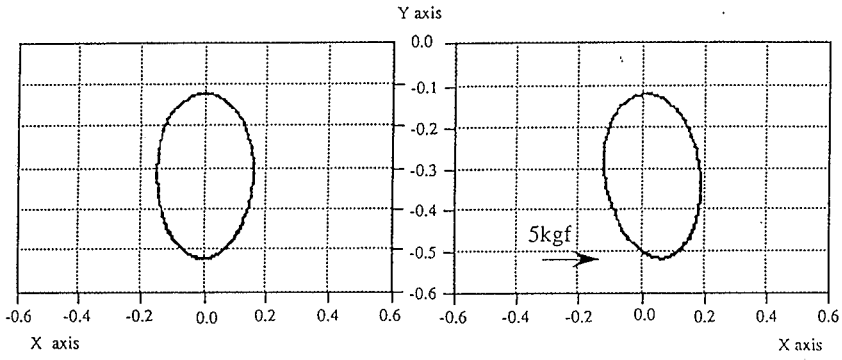


Fig. 8. Contour of the work space.

Note that Eq. (12) includes the passive joints $\boldsymbol{\phi}$ which are the functions of both the external force **F** and the angles of the active joints. First, we assume that the external force **F** is constant. As ϕ_0 is determined only by the external force **F**, $d\phi_0=0$ is obtained. Let the left term be substituted by $f(\phi_1, \theta_2, \theta_3, \theta_4)$. Then, because of the equilibrium of Eq. (6), we obtain

$$d\boldsymbol{\phi}=Nd\boldsymbol{\theta} \tag{13}$$

where

$$N=\begin{bmatrix} 0 & 0 & 0 \\ n_2 & n_3 & n_4 \end{bmatrix},\ n_i=-\frac{\partial f}{\partial \theta_i}\Big/\frac{\partial f}{\partial \phi_i}$$

From these results, Eq. (12) can be rewritten as

$$d\mathbf{x}=(J_\phi N+J_\theta)d\boldsymbol{\theta} \tag{14}$$

The Jacobian matrix of the wire suspended manipulator is obtained under the condition that a constant external force is applied.

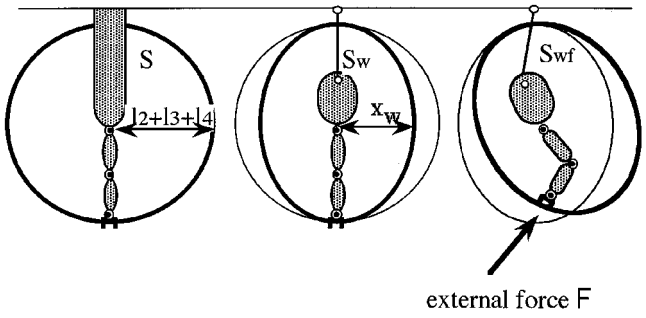


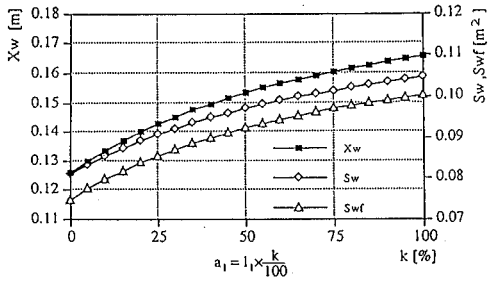
Fig. 9. Work space of a wire suspended manipulator and fixed base manipulator.

Table II. Standard link parameters

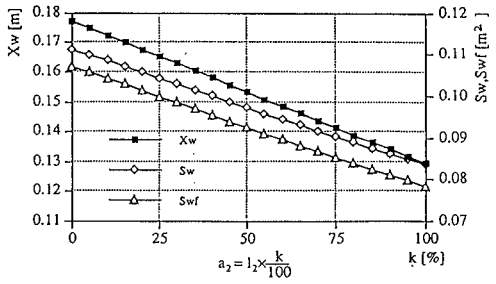
L_0 0.20 [m]		
L_1 0.12 [m]	a_1 0.06 [m]	m_1 3.40 [kg]
L_2 0.10 [m]	a_2 0.05 [m]	m_2 2.20 [kg]
L_3 0.10 [m]	a_3 0.05 [m]	m_3 0.70 [kg]

3.2 Solution of inverse kinematics

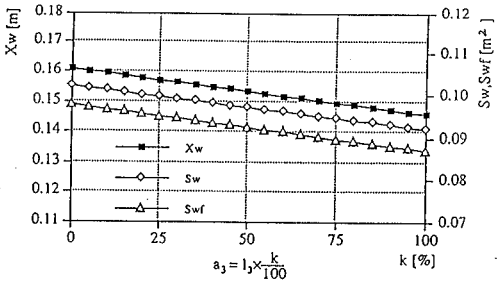
We can compute inverse kinematics of the wire suspended manipulator by means of an iterative calculation using the Jacobian matrix in Eq. (14).



(A) Relations between a_1 and Xw, Sw, Swf



(B) Relations between a_2 and Xw, Sw, Swf



(C) Relations between a_3 and Xw, Sw, Swf

Fig. 10. Relations between the center of gravity and Xw, Sw, Swf.

https://doi.org/10.1017/S0263574799000995 Published online by Cambridge University Press

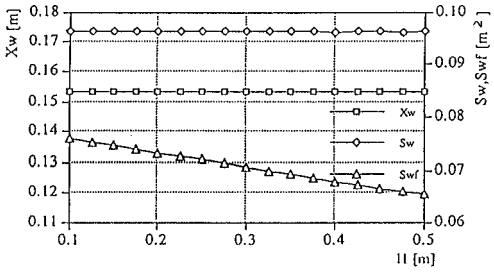


Fig. 11. Relations between L1 and Xw, Sw, Swf.

The inverse kinematics of the manipulator has two solutions except for the case of a singular configuration. These two are, however, different from the similar plural solutions of an ordinary serial links with 3 degrees of freedom. Those in this manipulator are not geometrically symmetrical as in Fig. 5. Hence, when we calculate the inverse kinematics, we should distinguish the case of $\theta_3 < 0$ from the case of $\theta_3 > 0$.

For the inverse kinematics by iterative computation, the initial pose affects the solutions and the computation time. When the pose of the end-effector and the external force are given, the initial pose is set in the following way:

(i) The angle ϕ_0 is calculated by Eq. 5.
(ii) With $\phi_1 = 0$, θ_1 are calculated by the pose of the end-effector.
(iii) From ϕ_0 and θ_1 determined above, ϕ_1 is calculated by Eq. (8).

When the initial value is taken as $\theta_3 < 0$, the solution may remain negative as $\theta_3 < 0$, and as $\theta_3 > 0$, the solution may be positive.

Using this algorithm, we simulated the inverse kinematics. The link parameters of the simulation are listed in Table I. The initial end-effector pose is $(-0.08, -0.30)$, the goal end-effector pose is $(0.05, -0.35)$, and the external force is 0. Simulation results are illustrated in Fig. 6. The left-hand figure in Fig. 6 is the result for $\theta_3 < 0$, and the right one is for $\theta_3 > 0$.

In Fig. 6, the sign of θ_2 changes in the case of $\theta_3 < 0$. This is inevitable, because the solution of inverse kinematics at the initial position can be realized only in the case of $\theta_2 < 0$. However, that at the goal position can be realized only in the case of $\theta_2 > 0$.

Let us define reachable space as the space where the end-effector of the wire suspended manipulator can move. The reachable space is illustrated in Fig. 7. The right-hand figure indicates the area on $\theta_2 > 0$, and the right-hand one does $\theta_2 < 0$. The union of these two represents the work space as illustrated at the center. Hence according to the initial and goal poses, the wire suspended manipulator has to pass through the configuration with singularity. This may be a disadvantage of this type of suspended system. However, the pose can be chosen so as to connect smoothly the initial pose to the goal pose, because the suspended manipulator usually has redundant degrees of freedom.

4. STATICS OF MANIPULATOR

The torque vector required for keeping the joint angles under external forces is calculated. From the principle of virtual work, Eq. (15) is obtained,

$$\mathbf{F}^T d\mathbf{r}_E + M\mathbf{g}^T d\mathbf{r}_g = \boldsymbol{\tau}^T d\mathbf{q} \tag{15}$$

where $\mathbf{q} = [\boldsymbol{\phi}^T \boldsymbol{\theta}^T]^T$, $\boldsymbol{\tau} = [0\ 0\ \tau_3\ \tau_4\ \tau_5]^T$.

$\boldsymbol{\tau}$ is a torque vector of the suspended manipulator. The first and the second elements of $\boldsymbol{\tau}$ are corresponding to the passive joints. From Eq. (12), the relationship between $d\mathbf{r}_E$ and $d\mathbf{q}$ can be expressed as Eq. (16) using a Jacobian matrix J_E.

$$d\mathbf{r}_E = J_E d\mathbf{q} \tag{16}$$

The relationship between $d\mathbf{r}_g$ and $d\mathbf{q}$ can also be expressed as Eq. (17) using a Jacobian matrix J_g.

$$d\mathbf{r}_g = J_g d\mathbf{q} \tag{17}$$

Substituting Eq. (16) and (17) into Eq. (15), Eq. (18) is obtained.

$$\mathbf{F}^T J_E d\mathbf{q} + M\mathbf{g}^T J_g d\mathbf{q} = \tau^T d\mathbf{q} \tag{18}$$

Thus, the torques required for each active joint can be derived as Eq. (19).

$$\boldsymbol{\tau} = J_E{}^T \mathbf{F} + M J_g{}^T \mathbf{g} \tag{19}$$

It can easily be proved that the first and the second elements of $\boldsymbol{\tau}$ become zero.

5. GUIDELINE OF DESIGNING A WIRE SUSPENDED MANIPULATOR

5.1 Work space of a wire suspended manipulator

5.1.1 Definition and solution of a work space. Reachable space of a wire suspended manipulator depends on the external force. Figure 8 shows the contour of the reachable space according to the external force. The reachable space has an ellipse-like shape with a narrower width along the X-axis than the shape of the reachable space of a fixed base manipulator. This is because the gravity center of the system is constrained on the Y-axis. With an external force applied to the end-effector, the ellipse leans in the direction of the external force. Assuming the external force as $\mathbf{F} = \alpha\mathbf{n}$ ($\mathbf{n}$ is a unit vector), let us define the workspace of a wire suspended manipulator as all of the intersection of the reachable space for $\mathbf{F} = t\mathbf{n} (0 < t < \alpha)$.

5.1.2 Relations between work space and link parameters. The work space of a wire suspended manipulator is determined by the kinematics of links, masses and an external force. Thus the design of the manipulator is completely different from an ordinary fixed-base manipulator. Since the work space of the wire suspended manipulator is usually smaller than that of an ordinary manipulator, we introduce the area of its work space as a criterion. Figure 9 shows the definitions of the area of reachable space S_w and the area of work space S_{wf}.

Since the reachable space of the wire suspended manipulator is similar to an ellipse, the maximal width of the x coordinates of the space of the fixed base manipulator X_w may have a strong relation to the amount of both S_w and S_{wf}. The x coordinate of the end-effector is represented as

https://doi.org/10.1017/S0263574799000995 Published online by Cambridge University Press

Table III. Standard link parameters

L_0	0.20 [m]				
L_1	0.20 [m]	a_1	0.10 [m]	m_1	1.61 [kg]
L_2	0.16 [m]	a_2	0.08 [m]	m_2	1.05 [kg]
L_3	0.16 [m]	a_3	0.08 [m]	m_3	1.65 [kg]

Eq. (9). However, from force constraints, the gravity center is constrained onto the axis as Eq. (20).

$$A_1S_1+A_2S_{12}+A_3S_{123}=0 \tag{20}$$

with

$$A_1=m_1a_1+(m_2+m_3)L_1,$$

$$A_2=m_2a_2+(m_3L_2,\ A_3=m_3a_3$$

The maximum X_w is calculated by Lagrange multiplier as Eq. (21).

$$X_w=L_2+L_3-\frac{A_2+A_3}{A_1L_1} \tag{21}$$

The values X_w, S_w and S_{wf} are computed against the various link parameters. The standard link parameters are listed in Table II. The relations between the work space and the link parameters are plotted in Figs. 10 and 11.

The equation (16) for calculating X_w is represented analytically. On the contrary, S_w and S_{wf} cannot be calculated directly. But as shown in Figs. 10, and 11, the characteristics of S_w and S_{wf} are similar to X_w. Hence it is efficient to evaluate X_w instead of S_{wf}.

5.2 Manipulability measure of a wire suspended manipulator

5.2.1 Manipulability ellipsoid and manipulability measure. Manipulability is often used for the evaluation of manipulators. When an end-effector velocity vector is **v**, the manipulability ellipsoid is represented as Eq. (22).

$$\mathbf{v}^T(J^+)^TJ^+\mathbf{v}\le 1 \tag{22}$$

And, the manipulability measure is scalar that can represent manipulability quantitatively as Eq. (23).

$$w=\sqrt{\det(J(\mathbf{q})J^T(\mathbf{q})} \tag{23}$$

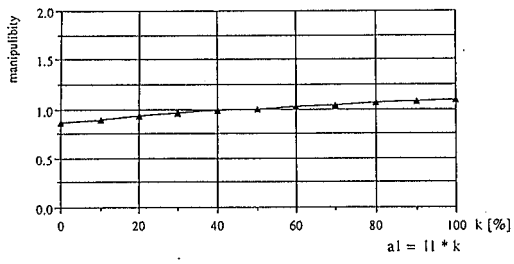
In a wire suspended manipulator, we can also define the manipulability ellipsoid and manipulability measure from the Jacobian matrix in Eq. (14).

5.2.2 Relations between manipulability measure and link parameters. Let us calculate manipulability through the link parameters of the wire suspended manipulator. The standard link parameters are given in Table III, which defines the normal value of a manipulability measure. The relations between the manipulability measure and link parameters are shown in Fig. 12 and 13.

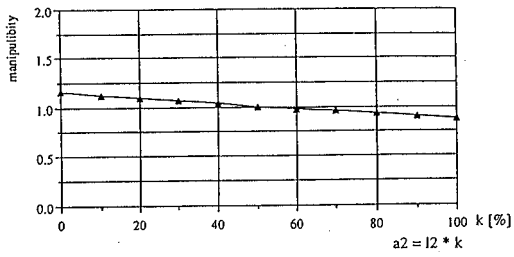
From Fig. 12, the result of the manipulability measure is similar to that of the work space. So if we design the link parameters to enlarge the work space, the manipulability measure also becomes large. With regard to the link length, Fig. 13(b) implies that if L_2 is equal to L_3, the manipulability measure is larger.

5.3 Guidelines of designing a wire suspended manipulator

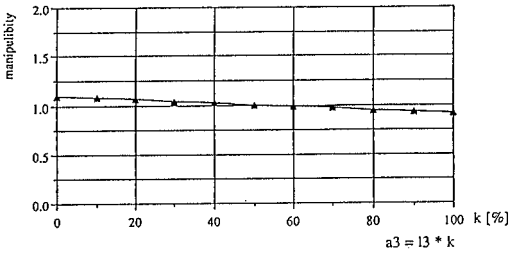
In Section 4.2, we found that a large work space leads to a large manipulability measure. And in Section 4.1, it is effective to evaluate X_w on behalf of S_{wf} in order to enlarge the work space. From Eq. (16), the larger a_1, the smaller a_2 and a_3 makes X_w larger. In a similar analysis, the larger m_1, the smaller m_2 and m_3 makes X_w larger. These results show that when the center of gravity of the total system is set near to the first active joint, the change of configuration does not affect the position of the center of gravity. In short, the nearer the gravity center of the system is to the first active joint, the larger X_w is. In other words, a large and heavy first link allows the other front-side links to move freely without



(A) Relations between a_1 and manipulability measure



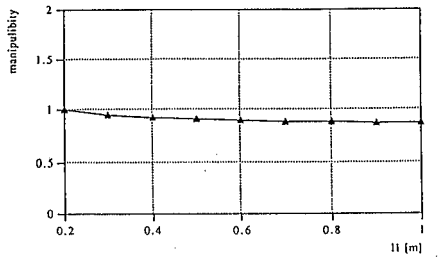
(B) Relations between a_2 and manipulability measure



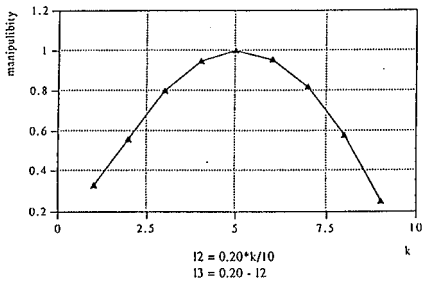
(C) Relations between a_3 and manipulability measure

Fig. 12. Relations between the center of gravity and manipulability measure.

https://doi.org/10.1017/S0263574799000995 Published online by Cambridge University Press



(A) Relations between L_1 and manipulability measure



(B) Relations between L_2, L_3 and manipulability measure

Fig. 13. Relations between link length and manipulability measure.

a change of the center of gravity. If the gravity center of the system is on the first active joint, the work space of a wire suspended manipulator is just equal to work space of a fixed-base manipulator because the gravity center of the system is decided without the motion of active joints.

6. CONCLUSION

To enlarge the work space of manipulators, we propose a wire suspended manipulator, which consists of a serial link, wire suspension mechanism and a crane system. The kinematics of the mechanism is obtained and studied.

(i) In modeling a wire suspension as a rigid link with passive joints at both ends of the wire, the kinematics and Jacobian matrix are obtained from the angles of the active joints and force constraints by gravity.

(ii) The characteristics of the wire suspended manipulator are studied. The work space and reachable space are obtained.

(iii) The guidelines in the design of a wire suspended manipulator are studied by simulations.

The dynamic motion control and the planning of compliant motions will be studied in future work. When fast motions are required for the manipulator, the wire tension may become negative due to the dynamic effect of the manipulator. As a result, the control system may become unstable. When the manipulator collides with an unexpected environment during assembly tasks, the system may also become unstable due to the discontinuous change of control models. Thus, these two items are key technical issues during the practical use of this system.

References

1. H. Seraji, “Configuration Control of Rober-Mounted Manipulators” *Proc. IEEE Int. Conf. on Robotics and Automation* (1995) **Vol. 2**, pp. 2261–2266.
2. W. Miksh and D. Schroeder, “Performance-Functional Based Controller Design for a Mobile Manipulator” *Proc. 1992 Int. Conf. of Robotics and Automation* (1992) **Vol. 1**, pp. 227–232.
3. Y. Yamamoto and X. Yun, “Coordinating Locomotion and Manipulation of a Mobile Manipulator” *IEEE Trans, on Automatic Control* **39**, No. 6, 1326–1332 (1994).
4. N. Koyachi, T. Arai, H. Adachi, K. Asami and Y. Itoh, “Hexapod with Integrated Limb Mechanism of Leg and Arm” *Proc. of 1995 IEEE Int. Conf. on Robotics and Automation* (1995) pp. 1952–1957.
5. Matthew M. Cusack and J.G. Thomas, “Wall Climbing Robots for Inspection in Vertical Environments” *Proc. 24th Int. Symp. on Ind. Robots* (1993) pp. 495–502.
6. F. Saito, T. Fukuda and F. Arai, “Swing and Locomotion Control for Two-Link Brachiation Robots” *IEEE Int. Conf. on Robotics and Automation* (1993) **Vol. 2**, pp. 719–724.
7. Y. Umetani and K. Yoshida, “Resolved Motion Rate Control of Space Manipulators with Generalized Jacobian matrix” *IEEE Trans. on Robotics and Automation* **5**, No. 3, 303–314 (1989).
8. Y. Nakamura and R. Iwamoto, “Stabilization of the Shape of Space Multibody Structure with Free Joints” *IEEE/RSJ Int. Conf. on IROS* (1993) **Vol. 3**, pp. 2095–2101.
9. T. Arai, H. Osumi and H. Yamaguchi, “Assembly Robot Suspended by Three Wires with Seven Degrees of Freedom”, MS90–807, *Proc. 11th Int. Conf. on Assembly Automation*, (1990) pp. MS90–807 - 1/13.
10. H. Osumi, T. Arai and H. Asama, “Development of a Crane Type Root with Three Wires” *Proc. 23rd Int. Symp. Ind. Robots* (1992) pp. 561–566.

https://doi.org/10.1017/S0263574799000995 Published online by Cambridge University Press